Subcellular Distribution of the 1,4-Dihydropyridine Receptor in Rabbit Skeletal Muscle In Situ:
An Immunofluorescence and Immunocolloidal Gold-labeling Study

Annelise O. Jorgensen,* Amy C-Y. Shen,* Wayne Arnold,* Albert T. Leung,‡ and Kevin P. Campbell‡

*Department of Anatomy, University of Toronto, Toronto, Canada M5S 1A8; and ‡Department of Physiology and Biophysics, University of Iowa, Iowa City, IA 52242

Abstract. The subcellular distribution of the 1,4-dihydropyridine receptor was determined in rabbit skeletal muscle in situ by immunofluorescence and immunoelectron microscopy. Longitudinal and transverse cryosections (5–8 μm) of rabbit gracilis muscle were labeled with monoclonal antibodies specific against either the α_1-subunit (170,000-D polypeptide) or the β-subunit (52,000-D polypeptide) of the 1,4-dihydropyridine receptor by immunofluorescence labeling. In longitudinal sections, specific labeling was present only near the interface between the A- and I-band regions of the sarcomeres. In transverse sections, specific labeling showed a hexagonal staining pattern within each myofiber however, the relative staining intensity of the type II (fast) fibers was judged to be three- to fourfold higher than that of the type I (slow) fibers. Specific immunofluorescence labeling of the sarcolemma was not observed in either longitudinal or transverse sections. These results are consistent with the idea that the α_1-subunit and the β-subunit of the purified 1,4-dihydropyridine receptor are densely distributed in the transverse tubular membrane.

Immunoelectron microscopical localization with a monoclonal antibody to the α_1-subunit of the 1,4-dihydropyridine receptor showed that the 1,4-dihydropyridine receptor is densely distributed in the transverse tubular membrane. Approximately half of these were distributed in close proximity to the junctional region between the transverse tubules and the terminal cisternae. Specific labeling was also present in discrete foci in the subsarcolemmal region of the myofibers. The size and the nonrandom distribution of these foci in the subsarcolemmal region support the possibility that they correspond to invaginations from the sarcolemma called caveolae. In conclusion, our results demonstrate that the 1,4-dihydropyridine receptor in skeletal muscle is localized to the transverse tubular membrane and discrete foci in the subsarcolemmal region, possibly caveolae but absent from the lateral portion of the sarcolemma.

VOLTAGE-SENSITIVE Ca^{2+} channels are present in smooth, cardiac, and skeletal muscle as well as in neuronal and endocrine cells (35, 43). The 1,4-dihydropyridines are potent blockers of the L-type voltage-sensitive Ca^{2+} channels (14). Electrophysiological studies have shown that 1,4-dihydropyridine-sensitive Ca^{2+} channels are localized to the transverse tubule membrane in adult skeletal muscle (37). Binding studies have shown that high affinity receptors for the 1,4-dihydropyridines are enriched in isolated transverse tubular membranes (9) and isolated triads (25) from skeletal muscle, but constitute only 0.1–0.8% of the total protein in purified transverse tubular membrane vesicles (4, 9). Recently, it has been shown that dihydropyridines also inhibit charge movement in the transverse tubular membrane and thus excitation–contraction coupling in skeletal muscle (36).

The molecular properties of the dihydropyridine receptor from skeletal muscle has been extensively studied during the last few years and reviewed recently (3, 4, 12). The purified dihydropyridine receptor from skeletal muscle has been shown to contain at least four polypeptide components:

α_1-subunit, α_2-subunit, β-subunit, and γ-subunit. The α_1-subunit has an apparent molecular mass of 155–200 kD on SDS-PAGE under both nonreducing and reducing conditions and contains binding sites for dihydropyridine and arylalkylamine Ca^{2+} channel blockers. The primary amino acid sequence of the α_1-subunit is consistent with it being the ion conduction and voltage-sensing unit of the Ca^{2+} channel. The α_2-subunit has an apparent molecular mass of 165–175 kD under nonreducing conditions and 135–150 kD after reduction of disulfide bonds. The change in molecular mass is possibly due to dissociation of one or more disulfide linked proteins of 24–33 kD which have been referred to as the δ-subunits. The β-subunit of the dihydropyridine receptor has an apparent molecular mass of 50–61 kD on SDS-PAGE which is insensitive to reduction. The α_1-subunit and β-subunit are substrates for various protein kinases. The γ-subunit of the dihydropyridine receptor is a glycoprotein with an apparent molecular mass of 30–33 kD on SDS-PAGE. A stoichiometric ratio of 1:1:1:1 has been obtained for the α_1, α_2, β, and γ-subunits, respectively, after taking into consideration the glycoprotein nature of the α_2-subunit. This obser-

135

vation strongly suggests that all four subunits are integral components of the 1,4-dihydropyridine receptor.

In this paper, we report on the subcellular distribution of the α_1- and β-subunits of the purified 1,4-dihydropyridine receptor of adult rabbit skeletal muscle as determined by immunofluorescence and immunoelectron microscopical studies.

Materials and Methods

Monoclonal Antibodies to the 1,4-Dihydropyridine Receptor

The mAbs to the 170,000-D (α_1) and the 52,000-D (β) subunits of the 1,4-dihydropyridine receptor from rabbit skeletal muscle were prepared and characterized as previously described (24, 25). Immunoblotting was performed according to the methods of Towbin (42) using 5% non-fat dry milk in PBS (BLOTTO) for blocking and washing of the immunoblots as described (15). Determination of the immunoglobulin class of the mAbs was carried out by immunodiffusion according to the procedure of Ouchterlony (29). Each of the mAbs was immunodiffused against monospecific antibodies to mouse IgG$_1$, IgG$_{2a}$, IgG$_{2b}$, IgG$_3$, and IgM. mAb IIID5 to the α_1-subunit of the 1,4-dihydropyridine receptor used for immunoelectron microscopy was purified from the mouse ascites fluid by DEAE-Affi Gel Blue chromatography (1).

Monoclonal Antibodies to the Ca^{2+}-ATPase of the Sarcoplasmic Reticulum

mAb IID8 to the Ca^{2+}-ATPase from canine cardiac sarcoplasmic reticulum and mAb IIH11 to the Ca^{2+}-ATPase of rabbit skeletal sarcoplasmic reticulum used in this study were prepared, purified, and characterized as previously described (18).

Preparation of Skeletal Muscle Extract, Triads, and Transverse Tubule Membranes

The extract represents the supernatant obtained from tissue homogenates during the preparation of triads. Triads were prepared as described by Mitchell et al. (28) with slight modification (39). Transverse tubular membranes were prepared by the method of Rosemblatt et al. (34). Protein concentrations were determined by the method of Lowry (26) as modified by Peterson (31) using BSA as a standard. SDS-PAGE on 3–12% gradient gels was performed by the method of Laemmli (23).

Dissection, Fixation, and Sectioning

Fixed and unfixed bundles of skeletal muscle fibers from rabbit gracilis and psoas muscle were prepared as previously described (20). Briedfly, bundles of myofibers from rabbit gracilis or psoas muscle were dissected and quickly frozen in liquid nitrogen–cooled isopentane. Bundles of myofibers to be fixed were dissected from rabbit gracilis or psoas muscle and immediately tied to applicator sticks (for chemical fixation) or stainless steel loops (for cyrofixation) at 100–120% of their rest length and allowed to recover for 30 min in a modified Krebs-Henseleit buffer (145 mM NaCl, 2.6 mM KCl, 5.9 mM CaCl$_2$, 1.2 mM MgSO$_4$, 25 mM NaHCO$_3$, and 10 mM glucose, saturated with a mixture of 95% O$_2$ and 5% CO$_2$). The bundles of myofibers to be used for immunofluorescence studies were fixed for 3 h in ice-cold 2% paraformaldehyde in 0.1 M sodium cacodylate (pH 7.4). Sucrose infusion, storage, and cryosectioning (6–8 μm) were carried out as previously described. The bundles of myofibers to be used for immunocolloidal gold labeling were cryofixed, freeze-dried, and low temperature embedded in Lowicryl K4M as previously described (Procedure II [17]) except that 10 min before freezing, the Krebs-Henseleit buffer was changed to also include 4% polyvinyl pyrrolidone (Sigma Chemical Co., St. Louis, MO) as a cryoprotectant (19). Briefly the bundles of myofibers were cryofixed using the "Gentleman Jim" freezing device (Ted Pella, Tustin, CA) as described by Philips and Boyne (32). The cryofixed tissue was then quickly transferred to liquid nitrogen and stored overnight. Freeze-drying was carried out at low temperature in a glass cryosorption pump (5, 27). Infiltration and embedding of the cryofixed, freeze-dried tissue in Lowicryl K4M was performed according to the procedure of Chiovetti et al. (5, 6) as modified by Jorgensen

and McGuffee (17). Thin sections (60–80 nm) were collected on nickel grids coated with formvar.

Immunofluorescence Labeling

Immunofluorescence staining of cryosections from unfixed rabbit gracilis was carried out as previously described (20). The sections were first labeled with one of the following mAbs: IID8 to Ca^{2+}-ATPase of canine cardiac sarcoplasmic reticulum; IIH11 to Ca^{2+}-ATPase of rabbit skeletal sarcoplasmic reticulum; IIID5 and IIC12, to the α_1-subunit of the 1,4-dihydropyridine receptor; and VD2$_1$ to the β-subunit of the 1,4-dihydropyridine receptor. The secondary antibody was F(ab')$_2$ fragments of affinity-purified goat anti-mouse IgG conjugated to FITC (CooperBiomedical Inc., Malvern, PA). It was used at a dilution of 1:20. The fluorescence photographs were taken with a Zeiss photomicroscope provided with an Epi-fluorescence attachment and a phase-contrast condenser using Kodak Tri-X pan film.

Immunofluorescence staining of cryosections from fixed rabbit gracilis muscle were carried out as described for cryosections from unfixed rabbit gracilis muscle, except that the secondary antibody used above was substituted with a two-step incubation described below. After incubation with the primary antibodies, cryosections were washed in PBS (pH 7.4) and then incubated for 30 min with a 1:25 dilution of biotin conjugated to affinity-purified F(ab')$_2$ fragments of rabbit anti–mouse IgG (Jackson Laboratories, PA). Subsequently the sections were again washed in PBS (pH 7.4) and incubated for 30 min with a 1:100 dilution of FITC-conjugated streptavidin (Jackson Immuno Research Laboratories, Inc., Avondale, PA). Finally the sections were washed and mounted as previously described (20).

Histochemical Staining

Serial transverse sections of unfixed rabbit gracilis muscles were stained for myosin ATPase after alkaline preincubations (pH 10.4) as described by Guth and Samaha (13). This method specifically labels the myosin ATPase of only fast skeletal muscle fibers.

Immunocolloidal Gold Labeling

Immunocolloidal gold labeling of thin sections of cryofixed, freeze-dried, and Lowicryl K4M–embedded rabbit skeletal muscle was carried out as previously described (16, 17) except for the modification outlined below.

The sections were first labeled with DEAE-Affi-Blue gel–purified mAb IIID5 to the α_1-subunit of the 1,4-dihydropyridine receptor (15 μg/ml in PBS pH 7.4). Then an affinity-purified rabbit anti-mouse (Fc fragment) gamma globulin (Jackson Immuno Research Laboratories Inc.) was used at 25 μg/ml in PBS containing 3% BSA. Finally the sections were incubated with affinity-purified goat anti-rabbit gamma globulin–colloidal gold conjugate (3–7 nm) at 0.5 mg/ml PBS containing 3% BSA (Janssen Pharmaceutica, Beerse, Belgium).

To assess the immunolabeling specificity of the thin sections of Lowicryl K4M–embedded tissue, mouse gamma globulin purified from preimmune serum (10 μg/ml PBS) was substituted for mAb IIID5 in the immunolabeling procedure. After immunolabeling, the sections were first stained for 15 s in saturated uranyl acetate in 50% ethanol (6) and then for 15 s in lead citrate. The sections were examined in a Hitachi 7000 transmission electron microscope.

Ultrastructure of Cryofixed Tissue

To assess the preservation of the ultrastructural features of the cryofixed and freeze-dried skeletal muscle tissue used for the immunoelectron microscopical studies, some of these tissues were vapor osmicated and then embedded in Spurr resin, as described by McGuffee et al. (27). Thin sections were stained with 2% uranylacetate followed by lead citrate, according to standard procedures, and examined in a Hitachi 7000 transmission electron microscope.

Results

Characterization of mAbs to the α_1- and the β-Subunits of the 1,4-Dihydropyridine Receptor

It was previously shown by immunoblotting and immunoprecipitation experiments that mAb VD2$_1$ binds specifically to
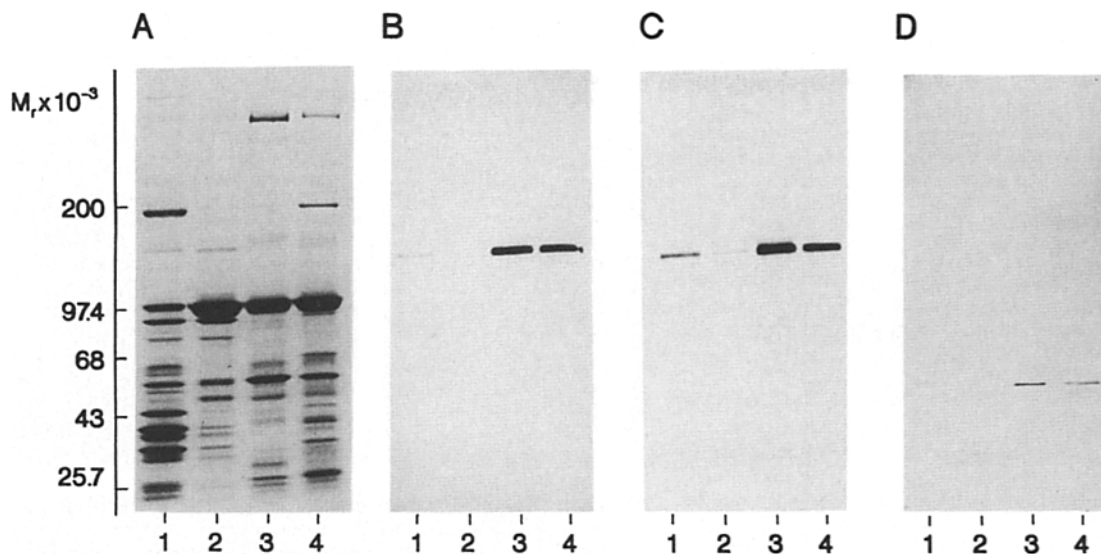
Figure 1. Coomassie Blue and immunoblot staining of rabbit skeletal muscle extract and membrane fractions. Rabbit skeletal muscle extract (lanes *1*), light sarcoplasmic reticulum membranes (lanes *2*), triads (lanes *3*), and transverse tubular membranes (lanes *4*) were prepared as described in Materials and Methods and separated on SDS-PAGE (30 μg/lane) followed by Coomassie blue staining or immunoblotting with monoclonal antibodies. *A* is a Coomassie blue–stained gel, *B, C,* and *D* are immunoblots of the gel stained with mAbs IIC12, IIID5, and VD2₁, respectively.

the β-subunit (52,000 D) of the 1,4-dihydropyridine receptor and that mAbs IIC12 and IIID5 bind specifically to the α₁-subunit (170,000 D) of the 1,4-dihydropyridine receptor. In the present study, the specificity of these antibodies toward the α₁- and β-subunits of the 1,4-dihydropyridine receptor was further demonstrated by their ability to bind only one polypeptide band on immunoblots of extracts from rabbit skeletal muscle (Fig. 1, *A–D*, lanes *1*). The mAb VD2₁ faintly stains a band in skeletal muscle extract (Fig. 1 *D*, lane *1*) that is difficult to visualize after photography. Both of the immunoreactive polypeptides are relatively enriched in isolated triads (Fig. 1, lanes *3*) and transverse tubular membranes (lanes *4*) and relatively depleted in light sarcoplasmic reticulum membranes (lanes *2*).

Distribution of the α₁- and the β-Subunits of the 1,4-Dihydropyridine Receptor in Type I (Slow) and Type II (Fast) Rabbit Gracilis Muscle

Serial transverse cyrosections from adult rabbit gracilis muscle containing a mixture of type I (slow) and type II (fast) myofibers were either labeled with mAb VD2₁ (anti–β-subunit) (Fig. 2 *a*) or with mAb IIC12 (anti–α₁-subunit) (Fig. 2 *b*) subunits of the 1,4-dihydropyridine receptor of rabbit skeletal muscle. To determine the fiber type distribution, additional serial cryosections were also stained with monoclonal antibodies specific for Ca²⁺-ATPase of the sarcoplasmic reticulum of either type I (slow) fibers (mAb IID8, Fig. 2 *d*) or type II (fast) fibers (mAb IIH11, Fig. 2 *e*) (18), and histochemically stained for the type II fiber marker alkali-stable actomyosin ATPase (Fig. 2 *f*) (13). One class of myofibers were weakly labeled with both mAb VD2₁ and mAb IIC12 and corresponded to the type I (slow) fibers. A second class of myofibers were strongly labeled with both mAb VD2₁ and with mAb IIC12 and corresponded to 95% of the type II (fast) fibers. A third class of myofibers constituting

~5% of the total fibers was also observed. This class of fibers was characterized by being more intensely labeled with mAb VD2₁ than the majority of the strongly labeled type II fibers but less intensely labeled with mAb IIC12 than the majority of the strongly labeled Type II fibers. Immunofluorescence labeling with another mAb IIID5 specific for the α₁-subunit of the 1,4-dihydropyridine receptor (Fig. 2 *c*) showed that 95% of the type II (fast) fibers also strongly labeled by mAb VD2₁ (anti–β-subunit) (Fig. 2 *a, star*) and mAb IIC12 (anti–α₁-subunit) (Fig. 2 *b, star*) were also strongly labeled with mAb IIID5 (Fig. 2 *c, star*) and that all type I (slow) fibers were weakly labeled with this antibody (Fig. 2 *c, solid circle*). However the intensity of labeling of the remaining 5% of type II (fast) and the type I (slow) fibers by mAb IIID5 was weak and indistinguishable from each other. The immunochemical and immunocytochemical characteristics of the mAbs used in the present report is summarized in Table I.

Comparison between the Distribution of the α₁- and the β-Subunits of the 1,4-Dihydropyridine Receptor in Skeletal Muscle Fibers

The studies described below were limited to type II (fast) myofibers. Examination of transverse sections of type II myofibers in gracilis muscle after immunolabeling with either mAb VD2₁ (anti–β-subunit) (Fig. 3 *a*) or with mAb IIID5 (anti–α₁-subunit) (Fig. 3 *f*) showed a polygonal staining pattern throughout the cytoplasm. The distance between the centers of neighboring polygons ranged from 1.1 to 1.5 μm. In contrast, the intensity of labeling of the sarcolemma was indistinguishable from that of the extracellular space. In longitudinal cyrosections of type II myofibers from fixed gracilis muscle, regular immunofluorescence staining with either mAb VD2₁ (anti–β-subunit) subunit (Fig. 3, *c, d,* and *e*) or with mAb IIID5 (anti–α₁-subunit) (Fig. 3, *h, i,* and *j*) ap-
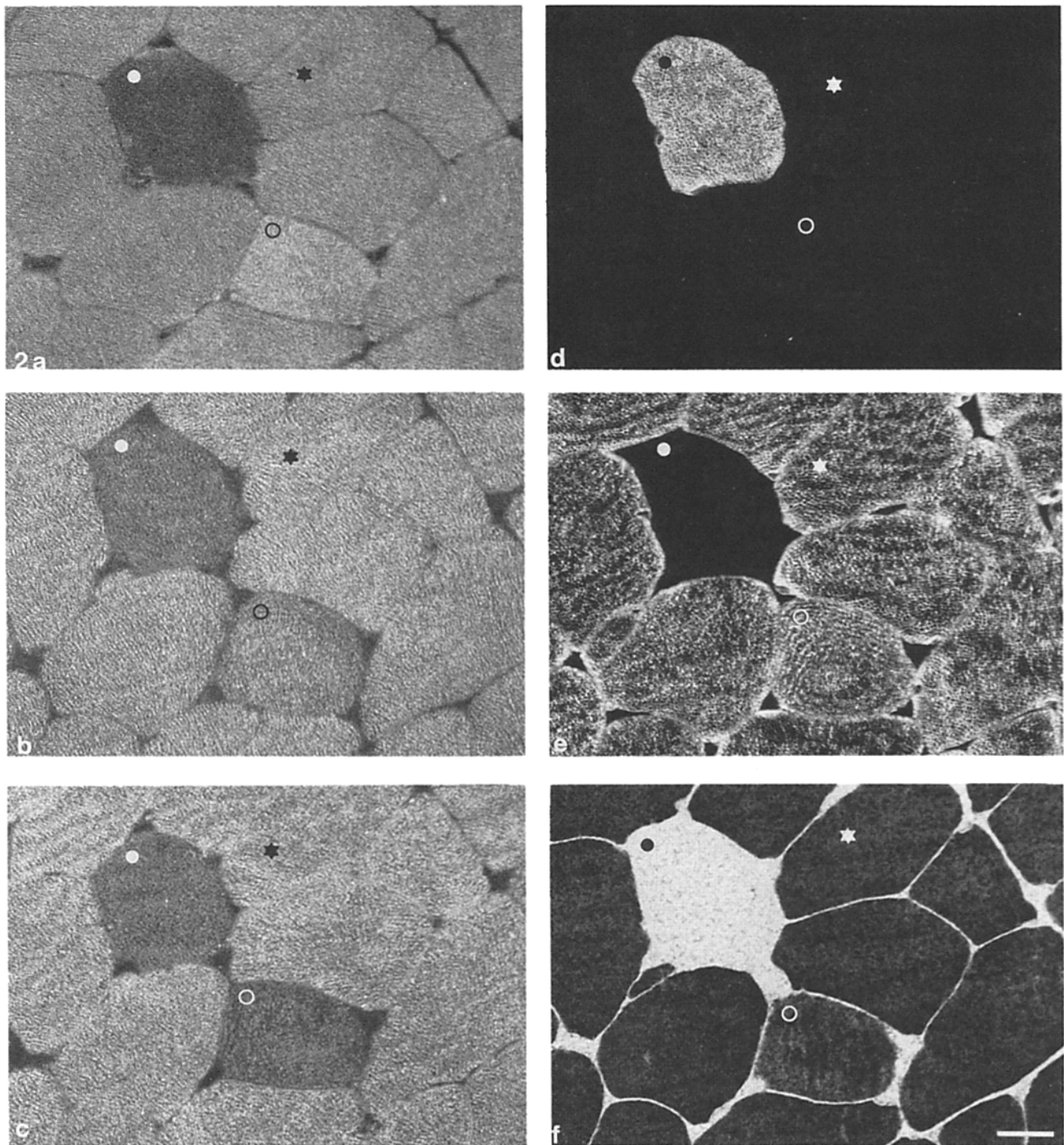
Figure 2. Distribution of the 52,000- and the 170,000-D subunit of the 1,4-dihydropyridine receptor in type I (slow) and type II (fast) myofibers of rabbit gracilis muscle. Serial transverse cryosections of unfixed rabbit gracilis muscle were immunofluorescently labeled with mAb VD2₁ (*a*) to the β-subunit of the 1,4-dihydropyridine receptor, with mAb IIC12 (*b*) and mAb IIID5 (*c*) to the α_1-subunit of the 1,4-dihydropyridine receptor, with mAb IID8 (*d*) and mAb IIH11 (*e*), respectively specific for the SR-Ca^{2+}-ATPase of the type I (slow) and type II (fast) myofibers of rabbit skeletal muscle and histochemically stained for alkali-stable myosin ATPase (*f*), a marker for type II (fast) myofibers. Note that three classes of fibers can be distinguished after labeling with either mAb VD2₁ (*a*), mAb IIC12 (*b*), or mAb IIID5 (*c*). One class is relatively intensely labeled with all three mAbs (*a*, *b*, and *c*, *star*); a second class is relatively weakly labeled with all three mAbs (*a*, *b*, and *c*, *solid circle*); a third class is more intensely labeled with mAb VD2₁ (*a*; *open circle*) but labeled with medium and low intensity by mAb IIC12 (*b*; *solid circle*) and mAb IIID5 (*c*; *solid circle*), respectively. The weakly labeled myofibers (*a*, *b*, and *c*, *solid circle*) correspond to type I (slow) fibers (*d*, *e*, and *f*, *solid circle*) while the remaining fibers correspond to type II (fast) fibers (*d*, *e*, and *f*, *star* and *open circle*). Bar, 20 μm.

Table I. Properties of Monoclonal Antibodies

Monoclonal antibody	Class*	Immuno-‡ PPT assay	Immunoblot‖ assay (M_r)	Immunocytochemical labeling of muscle fibers§		
					Type II		
				Epitope	95%	5%	Type I
			kD				
VD2₁	IgG₁	+	52	DHPR-subunit	+++	++++	+/-
IIC12	IgG₁	+	170	DHPR-subunit	+++	++	+/-
IIID5	IgG₁	+	170	DHPR-subunit	+++	+/-	+/-
IID8	ND		115	Ca²⁺-ATPase (cardiac, slow)	-	-	+++
IIH11	ND		115	Ca²⁺-ATPase (fast)	+++	+++	-

* Determination of the immunoglobulin class was carried out by immunodiffusion (13).
‡ The immunoprecipitation assay was performed as previously described (5).
§ The immunoblot assay was carried out as described in Materials and Methods.
‖ Fiber typing was determined according to the procedure of Guth and Samaha.
PPT, precipitation.
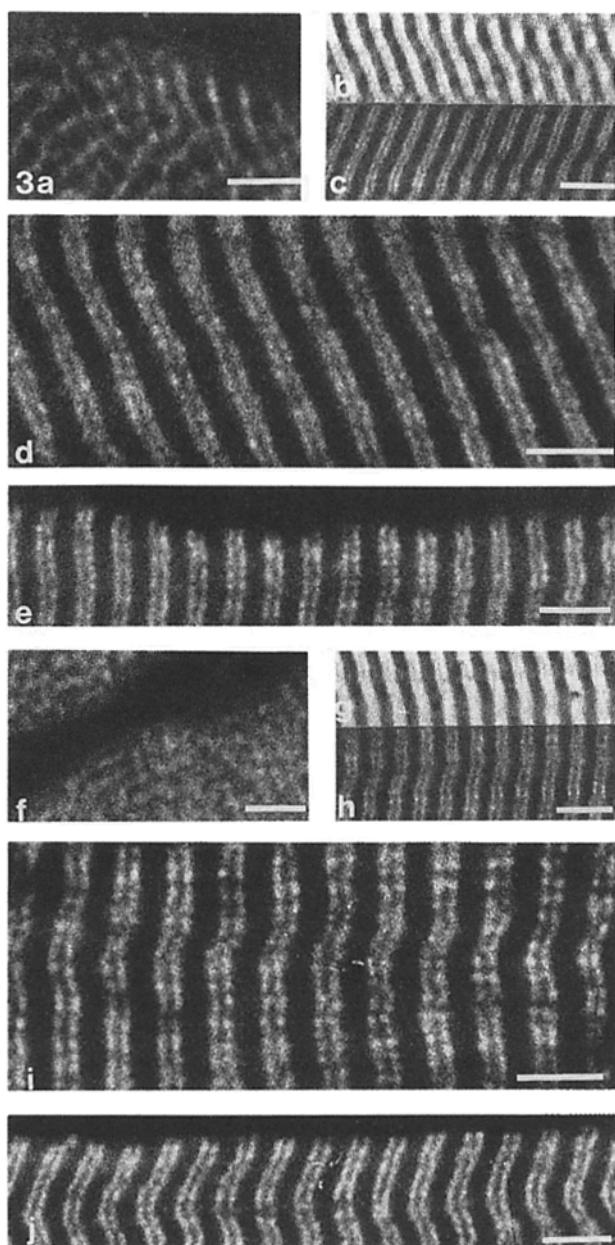
peared as transversely oriented rows of small bright foci. The subcellular distribution of the immunofluorescence labeling (Fig. 3, c and h) corresponded to the interphase between the A-band and the I-band as observed by viewing the same field by phase-contrast microscopy of skeletal muscle (Fig. 3, b and g). The intensity of immunofluorescence of the sarcolemma was indistinguishable from that of the extracellular space after labeling with either mAb VD2₁ (Fig. 3 e) or mAb IIID5 (Fig. 3 j). This is especially evident in the A-band regions of the sarcolemma, where demarcation of the sarcolemma is absent.

Immunoelectron Microscopical Labeling

The distribution of the α₁-subunit and the β-subunits of the 1,4-dihydropyridine receptor in rabbit skeletal muscle fibers as determined by immunofluorescence labeling are consistent with the idea that both subunits of the 1,4-dihydropyridine receptor are densely distributed in the transverse tubular membrane but apparently absent from the sarcolemma.

Figure 3. Subcellular distribution of the 52,000- and the 170,000-D subunits of the 1,4-dihydropyridine receptor in type II myofibers of rabbit gracilis muscle. Unfixed (a and f) and fixed (2% paraformaldehyde) (b–e and g–j) adult rabbit gracilis muscle was cryostat sectioned transversely (a and f) and longitudinally (b–e and g–j) and labeled with mAb (VD2₁) to the β-subunit (a, c, d, and e) and with mAb (IIID5) to the α₁-subunit (f, h, i, and j) of the 1,4-dihydropyridine receptor purified from the triad subfraction of skeletal muscle membranes. In transverse sections (a and f) a polygonal staining pattern was observed after labeling with antibodies to either the β-subunit (a) or the α₁-subunit (f) of the 1,4-dihydropyridine receptor. Specific labeling of the sarcolemma was not apparent (a and f). The immunofluorescence staining pattern in c and h were compared with the position of the A- and I-bands in the same respective fields (mirror image) (b and g) as viewed by phase contrast microscopy. Regular fluorescent staining appeared as small bright foci in the interphase between the A- and I-bands after labeling with mAbs to either the β-subunit (c, d, and e) or the α₁-subunit (h, i, and j) of the 1,4-dihydropyridine receptor, however the intensity of labeling of the sarcolemma was generally indistinguishable from that of the extracellular space (e and j). Bar, 5 μm.
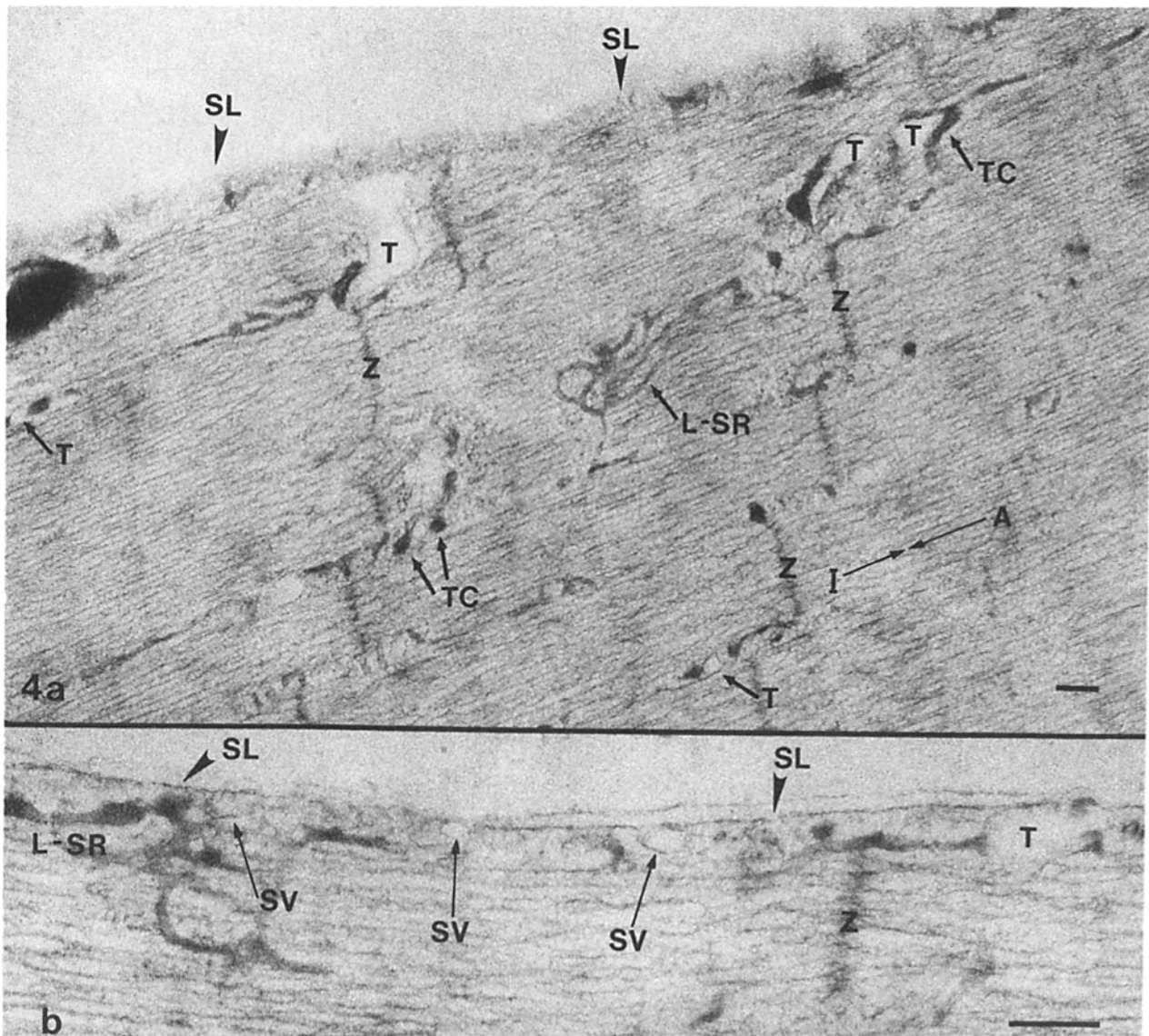
Figure 4. Ultrastructural features of longitudinal sections of rabbit skeletal muscle fibers. The tissue was cryofixed, freeze-dried, vapor fixed with osmium tetroxide, and embedded in Spurr (see Materials and Methods). A- and I-bands (*A*, *I* in *a* and *c*), Z-lines (*Z, a–d*), transverse tubules (*T, a–d*), longitudinal sarcoplasmic reticulum (*L-SR, a–d*), terminal cisternae (*TC, a, c,* and *d*), sarcolemma (*SL, a* and *b*), and subsarcolemmal vesicles (*SV, b*) are easily identified. Despite distortion of the arrangement of myofilaments in the myofibril due to ice crystal formation ultrastructurally distinct regions of the SR are well preserved (*a, c,* and *d*). Although the diameter of the T-tubules is considerably larger than normal the junctional complex between the T-tubules and the terminal cisternae is generally well preserved (*c* and *d*). Bars: (*a* and *b*) 0.2 μm; (*c* and *d*) 0.1 μm.

To determine more precisely the distribution of the 1,4-di-hydropyridine receptor, these studies were extended to include the immunoelectron microscopical localization of the α_1-subunit of the 1,4-dihydropyridine receptor in rabbit psoas muscle.

Preliminary studies showed that specific immunofluorescence labeling of the α_1-subunit of the 1,4-dihydropyridine receptor in skeletal muscle was eliminated when 0.3% glutaraldehyde was included in the 2% paraformaldehyde fixation solution. Since 2% paraformaldehyde both decreased the intensity of labeling and proved inadequate for the ultrastructural preservation of intracellular membranes in muscle tissue, it was not feasible to use ultrathin frozen sections for

immunolabeling. The loss of specific labeling after chemical fixation may in part be due to the low density of the 1,4-di-hydropyridine receptor in the transverse tubules (0.1–0.8% of total protein) (4, 9).

To optimize the preservation of the antigenicity and the in situ distribution of the 1,4-dihydropyridine receptor, the muscle tissue to be used for immunoelectron microscopical labeling was cryofixed, freeze-dried, and embedded in Lowicryl K4M (17). Since it is not feasible to osmicate the freeze-dried tissue before its low temperature embedding in Lowicryl K4M, visualization of membranes in the immunolabeled sections is variable and less than optimal. However, the position of T-tubules (*T*, Figs. 5, 6, and 7 *b*), terminal cisternae
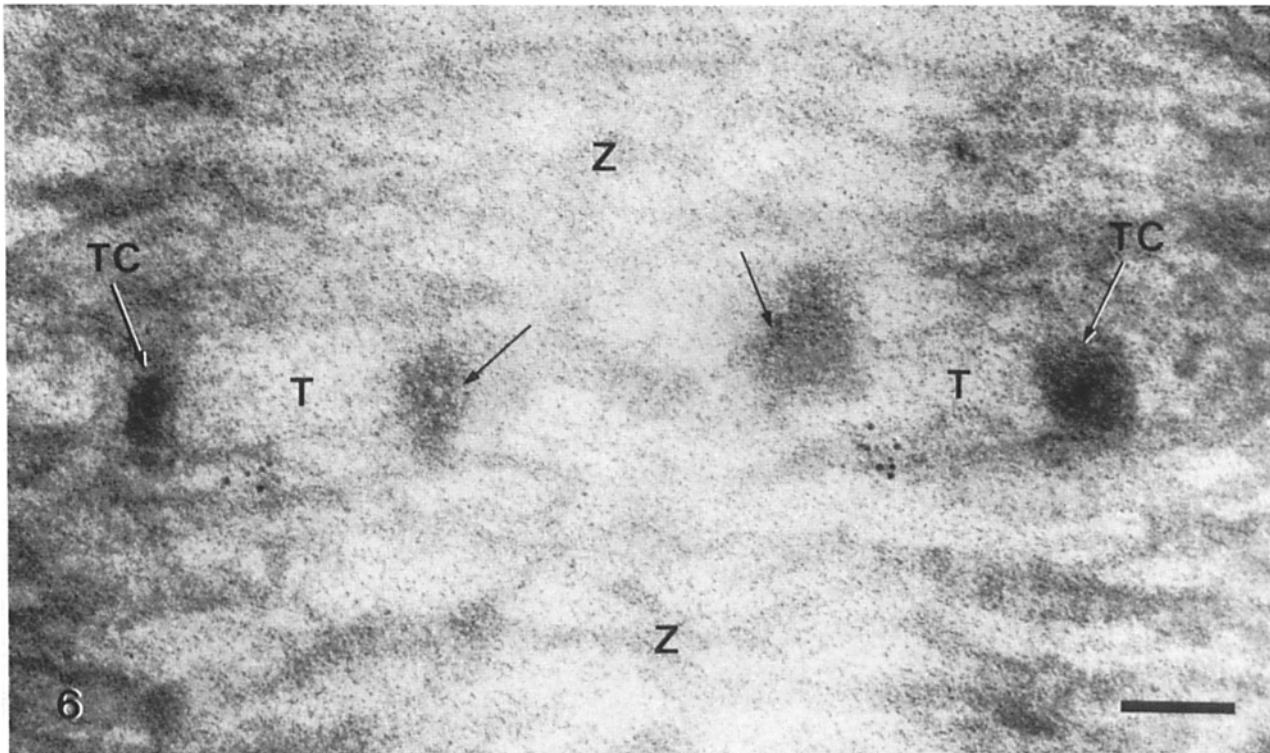
5
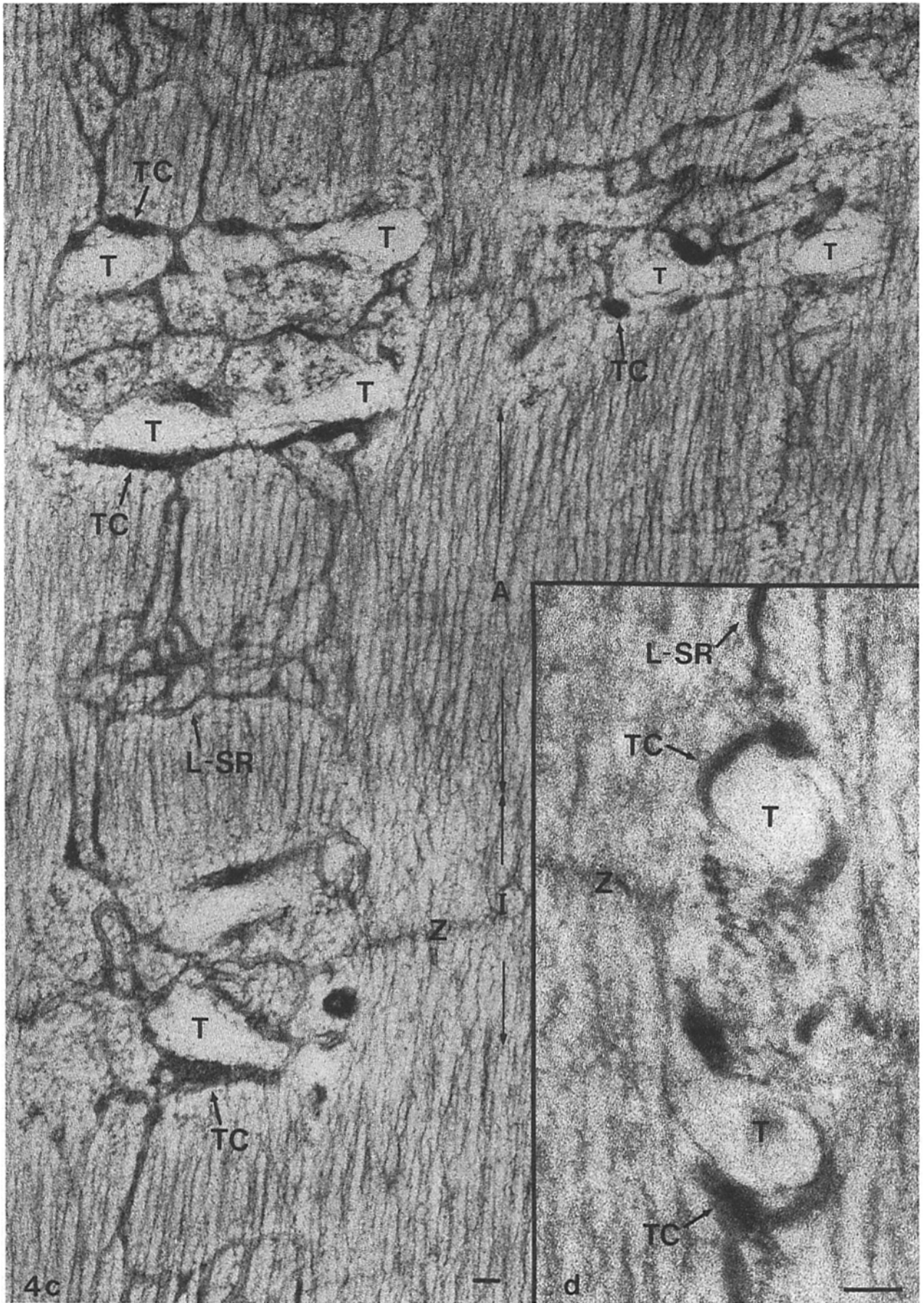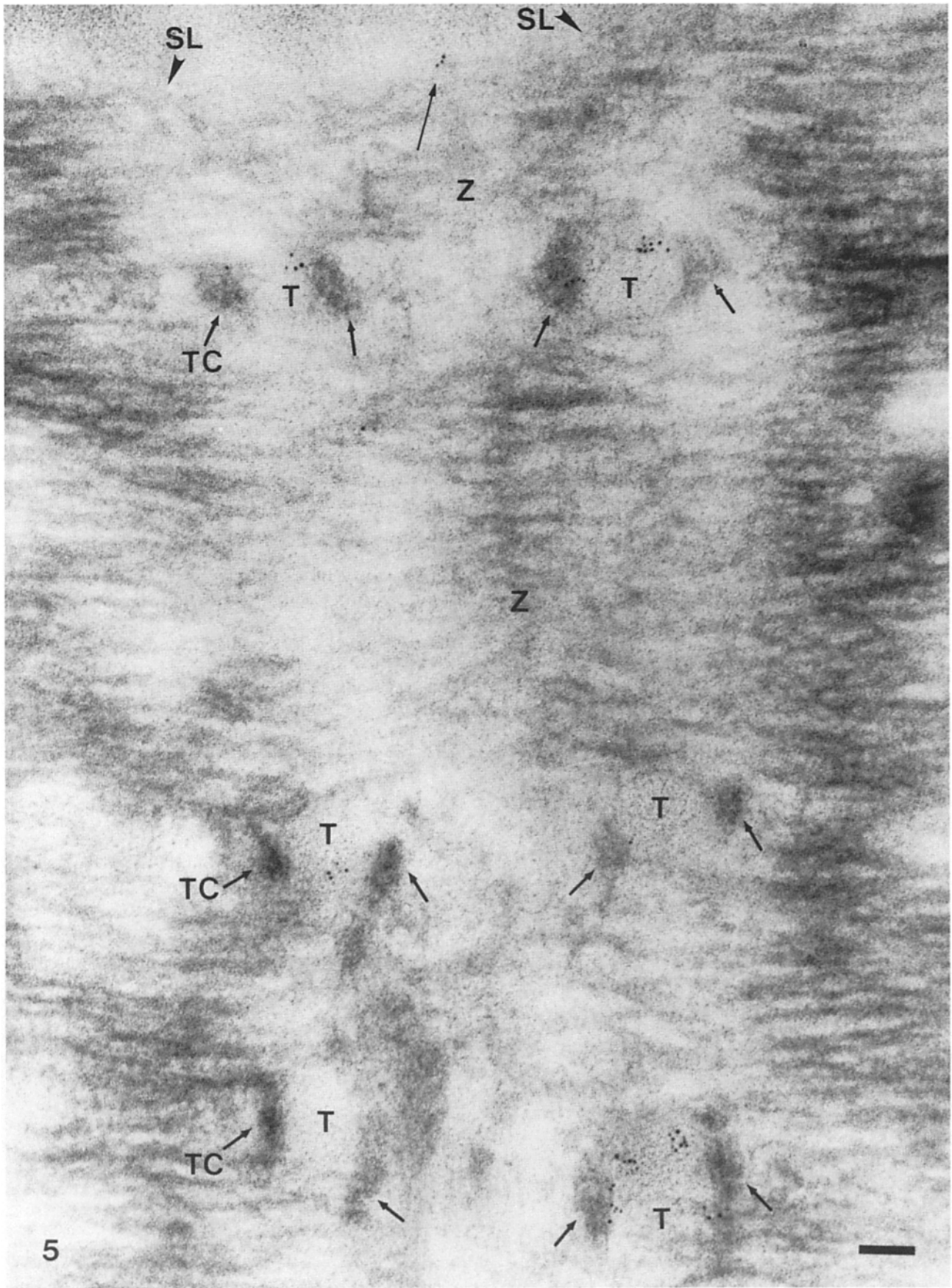
Figure 6. Electron micrograph of a longitudinal ultrathin section of rabbit skeletal muscle labeled with mAb IIID5 to the α_1-subunit of the 1,4-dihydropyridine receptor showing two triads. Colloidal gold particles are present over regions of the triads judged to correspond to T-tubular membrane (*T*) and absent from the terminal cisternae (*TC*) and the myofibrils. *Z*, Z-line. Bar, 0.1 μm.

(*TC*, Figs. 5, 6, and 7 *b*), and sarcolemma (*SL*, Figs. 5, 7, and 8) can readily be discerned. Subsarcolemmal vesicles and longitudinal sarcoplasmic reticulum are visualized very rarely unless the specimen is osmicated (Fig. 4).

To make sure that the sarcoplasmic reticulum, the transverse tubular, and the sarcolemmal membranes were well preserved, although not optimally visualized, some of the cryofixed and freeze-dried muscle tissues prepared for embedding in Lowicryl were instead vapor osmicated and Spurr embedded to permit visualization of membranes by positive staining. The ultrastructural features of the cryofixed, freeze-dried, osmicated, and Spurr-embedded tissue are shown in Fig. 4. Myofibrils are well preserved (Fig. 4 *a*). A- and I-bands (Fig. 4, *a* and *c*), as well as Z-lines (Fig. 4) can be readily identified. The darkly stained sarcoplasmic reticulum is well preserved throughout the section. Thus longitudinal SR (*L-SR*, Fig. 4) and the terminal cisternae (*TC*, Fig. 4, *a*, *c*, and *d*) were easily identified. Although the diameter of the T-tubules were enlarged (130–200 nm), most likely due to the hypertonic effect of the cryoprotectant, the T-tubular membrane was well preserved and closely apposed to the junctional sarcoplasmic reticulum (Fig. 4, *c* and *d*). The

sarcolemma (*SL*, Fig. 4 *b*) and subsarcolemmal vesicular structures (*SV*, Fig. 4 *b*) were also well preserved but only clearly visualized in sections obtained from the deeper regions of a cryofixed piece of muscle tissue where perpendicular sections through the sarcolemma can be obtained (Fig. 4 *b*). Sections obtained from the surface of the cryofixed tissue would mainly contain tangentially sectioned sarcolemma (Fig. 4 *a*).

Considering the fact that the resolution of the triple-layered immunocolloidal gold–labeling technique used is 70 nm, examination of the distribution of colloidal gold particles in rabbit skeletal muscle fibers showed that a majority of the gold particles were distributed over and within 35 nm of the perimeter of transverse tubules (Figs. 5, 6, and 7 *b*). Of these ∼50% were within 35 nm of the junctional region between the transverse tubule and the junctional sarcoplasmic reticulum. In addition, discrete clusters of colloidal gold particles were present in the subsarcolemmal region of the muscle fibers (Figs. 5, 7, *a* and *c*, and 8). Examination of several long sweeps of sarcolemma (Fig. 7, *a* and *b*) showed that the clusters of colloidal gold particles present in the subsarcolemmal region of the cell were distributed in a highly non-

Figure 5. Electron micrograph of a longitudinal section of cryofixed, freeze-dried, and Lowicryl K4M–embedded rabbit psoas muscle with mAb IIID5 specific for the α_1-subunit of the 1,4-dihydropyridine receptor by the triple-layered immunocolloidal gold–staining technique described in Materials and Methods section. Most of the colloidal gold particles were distributed over the lumen and the membrane of the transverse tubules (*T*). Occasionally, colloidal gold particles were distributed in the subsarcolemma region of the muscle fiber (*thin arrow*), while the sarcolemma (*SL*) and the terminal cisternae (*TC*; *thick arrows*) were generally labeled at the level of the background. Similarly, the myofibrils were also only labeled at the level of the background. *Z*, Z-line. Bar, 0.1 μm.
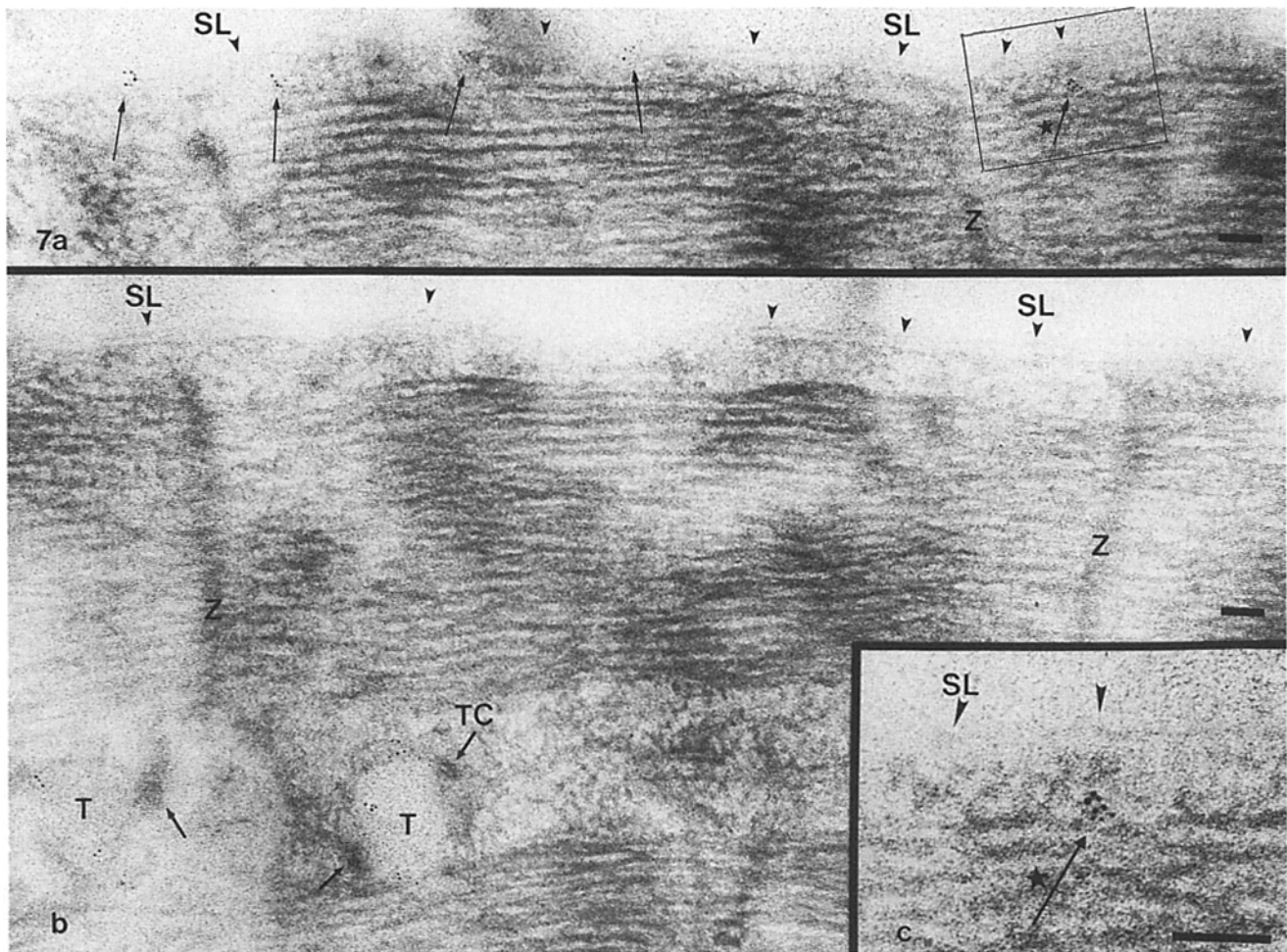
Figure 7. Electron micrographs showing two neighboring stretches of sarcolemma (*SL*) (*a* and *b*) in a longitudinal section of a rabbit skeletal myofiber immunolabeled with mAb IIID5 to the α_1-subunit of the 1,4-dihydropyridine receptor. Small clusters of colloidal gold particles are distributed in a highly nonrandom fashion in the subsarcolemmal region of the myofiber. Thus, while a particular stretch of subsarcolemma might contain several clusters of colloidal gold particles (*a, thin arrows*), a neighboring stretch of sarcolemma might contain no small clusters of colloidal gold particles in this region (*b*). However labeling of the transverse tubular membrane (*T*) present in the same section (*b*) was always observed. *c* is a higher magnification of the enclosed region shown in *a*. (*TC* and *thick arrows*) terminal cisternae; (*Z*) Z-line; (*SL, arrowheads*) sarcolemma. Bar, 0.1 μm.

random manner. Thus while extensive stretches of subsarcolemma might lack discrete clusters of gold particles (Fig. 7 *b*) neighboring stretches of sarcolemma in the same thin section of the same myofiber had a relatively high number of clusters per unit length of sarcolemma (Fig. 7 *a*). In contrast, colloidal gold particles were very sparsely distributed over the lateral regions of the sarcolemma (*SL*, Figs. 5, 7, *a* and *b*, and 8) (1 colloidal gold particle per 10 μm). Similarly, the myofibrils and the interfibrillar spaces where the sarcoplasmic reticulum is densly distributed were labeled at a level similar to that of the background (>1 colloidal gold particle per 10 μm^2).

Discussion

The 1,4-dihydropyridine receptor has been identified in many excitable and nonexcitable tissues by the binding of 1,4-dihydropyridines to tissue extracts or isolated membranes (14, 35, 37, 43). However, the subcellular distribution of this pro-

tein has not previously been described. This is the first report on the cellular and subcellular distribution of the 1,4-dihydropyridine receptor in rabbit skeletal muscle tissue in situ using immunocytochemical labeling.

The immunofluorescence labeling studies show that the α_1-subunit of the 1,4-dihydropyridine receptor is densely distributed in the interphase between the A- and I-bands in rabbit skeletal myofibers where the transverse tubules are located (10, 11) while apparently absent from the sarcolemma. This is in agreement with previous biochemical and pharmacological studies showing that the 1,4-dihydropyridine receptor is highly enriched in the isolated T-tubular membrane (9). Our finding that the distribution of the α_1-subunit is indistinguishable from that of the β-subunit of the 1,4-dihydropyridine receptor at the light microscopic level of resolution is consistent with the idea that the β-subunit is also confined to the transverse tubular membrane and is an integral component of the 1,4-dihydropyridine receptor.

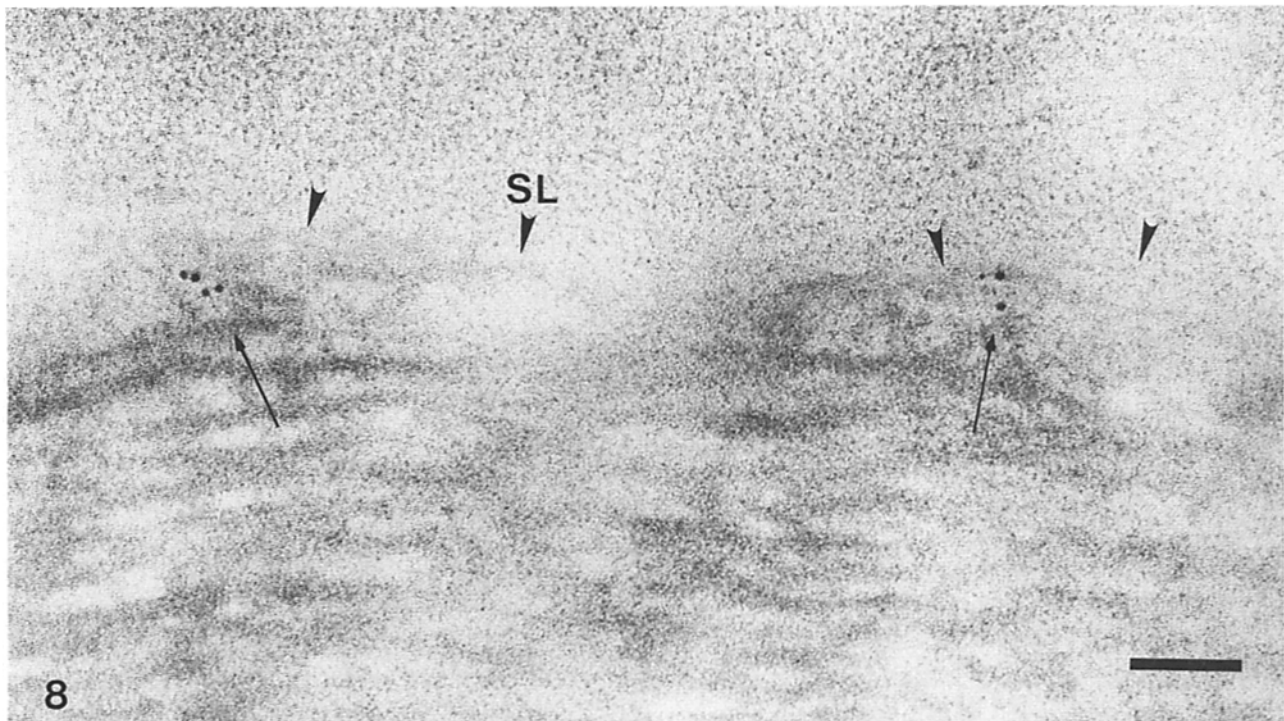The results of our immunofluorescence studies of trans-

Figure 8. Electron micrograph of a longitudinal section of rabbit skeletal muscle immunolabeled with mAb IIID5 to the α_1-subunit of the 1,4-dihydropyridine receptor and showing the peripheral region of this cell. Colloidal gold particles were associated with vesicular structures (*thin arrows*) present in the subsarcolemmal region of the myofiber. The sarcolemma (*SL* and *arrowheads*) was labeled only at the level of the background. Bar, 0.1 μm.

verse sections of rabbit gracilis muscle suggested that the intensity of labeling of both the α_1-subunit and the β-subunit is two- to threefold higher in 95% of the type II (fast) than in type I (slow) myofibers. This result might in part be explained on the basis of the twofold difference between the density of T-tubules of type II (fast) and type I (slow) myofibers as previously determined by morphometric analysis (8). Furthermore, this result is in good agreement with electrophysiological studies showing that the nifedipine inhibitable slow Ca^{2+} current is threefold higher in fast than that in slow skeletal muscle fibers of rat and rabbit (22). Finally, our immunofluorescence studies support the idea that the α_1-subunit and the β-subunit of the 1,4-dihydropyridine receptor are present in a constant stoichiometric ratio (24) in at least 95% of the myofibers of rabbit gracilis muscle.

If the α_1-subunit and the β-subunit of the 1,4-dihydropyridine receptor are indeed present in a 1:1 stoichiometric ratio as previously reported (24) our finding that 5% of the type II (fast) myofibers are more strongly stained with mAb VD2₁ to the β-subunit but more weakly stained with mAbs IIC12 and IIID5 to the α_1-subunit supports the possibility that distinct isoforms of these two subunits of the 1,4-dihydropyridine receptor exist. However further studies will be required to determine if this is indeed the case.

The immunoelectron microscopic studies showed that the α_1-subunit of the 1,4-dihydropyridine receptor is densely distributed over the transverse tubular membrane. Of these approximately half were distributed over the junctional region between the T-tubular membrane and the junctional sarcoplasmic reticulum. The results also showed that the α_1-subunit of the 1,4-dihydropyridine receptor was present

in discrete clusters in the subsarcolemmal region of skeletal myofibers but absent from the lateral regions of the sarcolemma. Although it is difficult to visualize membranes due to the specimen preparation procedure used, the discrete clusters of gold particles appeared occasionally to be membrane bound. We propose that the 1,4-dihydropyridine receptor containing foci in the subsarcolemmal region are membrane bound.

The localization of the 1,4-dihydropyridine receptor to the subsarcolemmal region of skeletal muscle by electron microscopy appears to be in disagreement with the results of the immunofluorescence studies presented here. This discrepancy could be explained by the nonuniform distribution of the 1,4-dihydropyridine receptor in the subsarcolemmal region of skeletal muscle and the limited sensitivity of the immunofluorescence technique. Although the 1,4-dihydropyridine receptor distributes in regular clusters in the subsarcolemmal region, the clusters might not have a sufficient concentration of 1,4-dihydropyridine receptor to permit detection by immunofluorescence.

Previously described membrane-bound structures present in the subsarcolemmal region of skeletal muscle fibers include caveolae (7, 30, 33, 34), transverse tubule openings to the sarcolemma (10, 44), junctional sarcoplasmic reticulum (40), and longitudinal sarcoplasmic reticulum. Since neither the longitudinal sarcoplasmic reticulum nor the terminal cisternae in the interior regions of the myofiber were labeled with antibodies to the α_1-subunit of the 1,4-dihydropyridine receptor, it seems unlikely that the colloidal gold–containing vesicular structures in the subsarcolemmal region of the myofiber correspond to either of these structures.

While direct continuity between transverse tubules and the sarcolemma has been difficult to demonstrate, ultrastructural studies of guinea pig (33) and frog skeletal muscle (44) showed that transverse tubules frequently terminate in caveolae which in turn are continuous with other caveolae and the sarcolemma. However physiological studies by Zampighi et al. (44) suggested that only a subgroup of the caveolae are connected with transverse tubules. Freeze-fracture studies have shown that caveolae are nonuniformly distributed on the cell surface in frog (7) and guinea pig skeletal muscle fibers (33). Since the size, shape, and nonuniform distribution of the α_1-subunit-containing entities in the subsarcolemmal region of rabbit skeletal muscle is similar to that described for caveolae (65 × 80 nm) (7) in other vertebrate skeletal muscles (33, 44) we propose that they represent caveolae, possibly the subgroup of caveolae connecting the transverse tubules and the sarcolemma (33, 44).

The exact physiological role of the 1,4-dihydropyridine receptor in skeletal muscle remains to be elucidated. Our finding that the α_1-subunit of the 1,4-dihydropyridine receptor is present in both the junctional and nonjunctional regions of the transverse tubular membranes as well as in subsarcolemmal entities proposed to be caveolae supports the possibility that this receptor has dual functions in skeletal muscle. It has been suggested that the 1,4-dihydropyridine receptor functions both as a voltage sensor in excitation–contraction coupling to release Ca^{2+} from the sarcoplasmic reticulum (36, 38, 41) and as a calcium channel (38, 41). Our finding that approximately half of the 1,4-dihydropyridine receptor labeling in the transverse tubular membranes is in close proximity to and thus potentially capable of communicating with the junctional sarcoplasmic reticulum membrane supports the hypothesis that these receptors act as voltage sensors in excitation–contraction coupling. Morphological data on transverse tubular membranes indicate that a distinctive set of intramembranous particles which are the sole components of the junctional transverse tubular membrane are present in diamond-shaped clusters that correspond exactly in position to the subunits of the "SR feet" (2). Our results support the contention that these particles are 1,4-dihydropyridine receptors. Preliminary results from our laboratory also suggest that a complex composed of the 1,4-dihydropyridine receptor and the ryanodine receptor can be isolated. All of these results suggest the presence of a large junctional complex, consisting of the 1,4-dihydropyridine and the ryanodine receptor, spanning the triadic junction and functioning in excitation–contraction coupling. Since the 1,4-dihydropyridine receptors in the nonjunctional region of the transverse tubules and in the caveolae are not in close proximity to the sarcoplasmic reticulum, it is unlikely that these receptors function as a sensor for excitation–contraction coupling. One possibility is that they function as calcium channels.

References

1. Bio-Rad Laboratories. 1983. DEAE Affi-Gel Blue Purifies IgG. BIORAD Bulletin 1062.
2. Block, B. A., T. Imagawa, K. P. Campbell, and C. Franzini-Armstrong. 1988. Structural evidence for direct interaction between the molecular components of the tubule/sarcoplasmic junction in skeletal muscle. *J. Cell Biol.* 107:2587–2600.
3. Campbell, K. P., A. T. Leung, and A. H. Sharp. 1989. The biochemistry and molecular biology of the dihydropyridine-sensitive calcium channel. *Trends Neurosci.* 11:425–430.
4. Catterall, W. A., M. J. Seagar, and M. Takahashi. 1988. Molecular properties of dihydropyridine-sensitive calcium channels in skeletal muscle. *J. Biol. Chem.* 263:3535–3538.
5. Chiovetti, R., L. J. McGuffee, S. A. Little, and J. Brass-Dale. 1987. Combined quick freezing, freeze-drying and embedding tissue at low temperature and in low viscosity resins. *J. Electron Microsc. Tech.* 5:1–15.
6. Chiovetti, R., L. J. McGuffee, S. A. Little, and J. Brass-Dale. 1985. A new approach for low-temperature embedding: quick freezing, freeze-drying and direct infiltration in Lowicryl K4M. *In* The Science of Biological Specimen Preparation for Microscopy and Microanalysis. M. Mueller, R. P. Becket, A. Boyde, and J. J. Wolosewick, editors. SEM Inc., AMF-O'Hare, Chicago, IL. 155–164.
7. Dulhunty, A. F., and C. Franzini-Armstrong. 1975. The relative contributions of the folds and caveolae to the surface membrane of frog skeletal muscle fibres at different sarcomere lengths. *J. Physiol.* 250:513–539.
8. Eisenberg, B. R. 1983. Quantitative ultrastructure of mammalian skeletal muscle. *Handb. Physiol.* 10:73–112.
9. Fosset, M., E. Jaimovich, E. Delpont, and M. Lazdunski. 1983. ^{3}H-Nitrendipine receptors in skeletal muscle. *J. Biol. Chem.* 258:6086–6092.
10. Franzini-Armstrong, C. 1973. Membranous systems in muscle fibers. *In* The Structure and Function of Muscle. Vol. 2. G. H. Bourne, editor. Academic Press, Inc., New York. 531–619.
11. Franzini-Armstrong, C., and K. R. Porter. 1964. Sarcolemmal invaginations constituting the T-system in fish muscle fibers. *J. Cell Biol.* 22:675–696.
12. Glossmann, H., and J. Striessnig. 1988. Structure and pharmacology of voltage-dependent calcium channels. *ISI Atlas Sci. Pharmacol.* 2:202–210.
13. Guth, L., and F. J. Samaha. 1969. Qualitative differences between actomyosin ATPase of slow and fast mammalian muscle. *Exp. Neurol.* 25:138–152.
14. Janis, R. A., and D. J. Triggle. 1984. 1,4-dihydropyridine Ca^{2+} channel antagonists and activators: a comparison of binding characteristic with pharmacology. *Drug Dev. Res.* 4:257–274.
15. Johnson, D. A., J. W. Gautsch, J. R. Sportsman, and J. H. Elder. 1984. Improved technique utilizing nonfat dry milk for analysis of proteins and nucleic acids transferred to nitrocellulose. *Gene Anal. Tech.* 1:3–8.
16. Jorgensen, A. O., and L. R. Jones. 1987. Immunoelectron microscopical localization of phospholamban in canine ventricular muscle. *J. Cell Biol.* 104:1343–1352.
17. Jorgensen, A. O., and L. J. McGuffee. 1987. Immunoelectron microscopic localization of sarcoplasmic reticulum proteins in cyrofixed, freeze-dried, and low temperature-embedded tissue. *J. Histochem. Cytochem.* 35:723–732.
18. Jorgensen, A. O., W. Arnold, D. R. Pepper, F. Mandel, S. D. Kohl, and K. P. Campbell. 1988. A monoclonal antibody to the Ca^{2+}-ATPase of cardiac sarcoplasmic reticulum cross-reacts with slow Type I but not with fast Type II canine skeletal muscle fibers: an immunocytochemical and immunochemical study. *Cell Motil. Cytoskeleton.* 9:108–116.
19. Jorgensen, A. O., R. Broderick, A. P. Somlyo, and A. V. Somlyo. 1988. Two structurally distinct calcium storage sites in rat cardiac sarcoplasmic reticulum. An electron microprobe analysis study. *Circ. Res.* 63:1060–1069.
20. Jorgensen, A. O., V. I. Kalnins, and D. H. MacLennan. 1979. Localization of sarcoplasmic reticulum proteins in rat skeletal muscle by immunofluorescence. *J. Cell Biol.* 80:372–384.
21. Deleted in proof.
22. Lamb, G. D., and T. Walsh. 1987. Calcium currents, charge movement and dihydropyridine binding in fast- and slow-twitch muscles of rat and rabbit. *J. Physiol. (Lond.).* 393:595–617.
23. Laemmli, U. K. 1970. Cleavage of structural proteins during the assembly of the head of bacteriophage T4. *Nature (Lond.).* 227:680–685.
24. Leung, A. T., T. Imagawa, B. Block, C. Franzini-Armstrong, and K. P. Campbell. 1988. Biochemical and ultrastructural characterization of the 1,4-dihydropyridine receptor from rabbit skeletal muscle. *J. Biol. Chem.* 263:994–1001.
25. Leung, A. T., T. Imagawa, and K. P. Campbell. 1987. Structural characterization of the 1,4-dihydropyridine receptor of the voltage-dependent Ca^{2+} channel from rabbit skeletal muscle. *J. Biol. Chem.* 262:7943–7946.
26. Lowry, O. H., N. J. Rosebrough, A. L. Farr, and R. J. Randall. 1951. Protein measurement with the folin phenol reagent. *J. Biol. Chem.* 193:265–275.
27. McGuffee, L. J., L. Hurwitz, S. A. Little, and B. E. Skipper. 1981. A

^{45}Ca autoradiographic and stereological study of freeze-dried smooth muscle of the guinea pig vas deferens. *J. Cell Biol.* 90:201–210.

28. Mitchell, R. D., P. Palade, and S. Fleischer. 1983. Purification of morphologically intact triad structures from skeletal muscle. *J. Cell Biol.* 96:1008–1016.

29. Ouchterlony, O. 1968. Handbook of Immunodiffusion and Immunoelectrophoresis. Ann Arbor Science Publishers, Ann Arbor, MI.

30. Peachey, L. D., and C. Franzini-Armstrong. 1983. Structure and function of membrane systems of skeletal muscle cells. *Handb. Physiol.* 10:23–71.

31. Peterson, G. L. 1977. A simplification of the protein assay method of Lowry et al. which is more generally applicable. *Anal. Biochem.* 83:346–356.

32. Phillips, T. E., and A. Boyne. 1984. Liquid nitrogen-based quick freezing: experiences with bounce-free delivery of cholinergic nerve terminals to a metal surface. *J. Electron Microsc. Tech.* 1:9–29.

33. Rayns, D. G., F. O. Simpson, and W. S. Bertaud. 1968. Surface features of striated muscle. II. Guinea-pig skeletal muscle. *J. Cell Sci.* 3:475–482.

34. Rosemblatt, M., C. Hidalgo, C. Vergara, and N. Ikemoto. 1981. Immunological and biochemical properties of transverse tubule membranes isolated from rabbit skeletal muscle. *J. Biol. Chem.* 256:8140–8148.

35. Reuter, H. 1983. Calcium channel modulation by neurotransmitters, enzymes and drugs. *Nature (Lond.).* 301:569–574.

36. Rios, E., and G. Brum. 1987. Involvement of dihydropyridine receptors in excitation-contraction coupling in skeletal muscle. *Nature (Lond.).* 325:717–720.

37. Sanchez, J. A., and E. Stefani. 1978. Inward calcium current in twitch muscle fibres of the frog. *J. Physiol. (Lond.).* 383:197–209.

38. Schwartz, L. M., E. E. McCleskey, and W. Almers. 1985. Dihydropyridine receptors in muscle are voltage-dependent but most are not functional calcium channels. *Nature (Lond.).* 314:747–750.

39. Sharp, A. H., T. Imagawa, A. T. Leung, and K. P. Campbell. 1987. Identification and characterization of the dihydropyridine-binding subunit of the skeletal muscle dihydropyridine receptor. *J. Biol. Chem.* 262:12309–12315.

40. Spray, T. L., R. A. Waugh, and J. R. Sommer. 1974. Peripheral couplings in adult vertebrate skeletal muscle. *J. Cell Biol.* 62:223–227.

41. Tanabe, T., H. Takeshima, A. Mikami, V. Flockerzi, H. Takahashi, K. Kangawa, M. Kojima, H. Matsuo, T. Hirose, and S. Numa. 1987. Primary structure of the receptor for calcium channel blockers from skeletal muscle. *Nature (Lond.).* 328:313–318.

42. Towbin, H., T. Staehelin, and J. Gordon. 1979. Electrophoretic transfer of proteins from polyacrylamide gels to nitrocellulose sheets: procedure and some applications. *Proc. Natl. Acad. Sci. USA.* 76:4350–4354.

43. Tsien, R. W. 1983. Calcium channels in excitable cell membranes. *Annu. Rev. Physiol.* 45:341–358.

44. Zampighi, G., J. Vergara, and F. Ramon. 1975. On the connection between the transverse tubules and the plasma membrane in frog semitendinosus skeletal muscle. *J. Cell Biol.* 64:734–740.